Effect of Osmolytes of Different Type on DNA Behaviour in Aqueous Solution. Experimental and Theoretical Studies.

Paulina W. Rakowska, Mateusz Kogut, Jacek Czub, Janusz Stangret

Abstract

Osmolytes, the small organic molecules accumulated in cells under environmental stress, can modulate the stability of biopolymers such as proteins and DNA. In spite of many years of research, there is no established molecular mechanism of the influence of osmolytes on DNA structure. Here, we used two model osmolytes that denature (urea) or stabilize (trimethylglycine, TMG) proteins to study their effect on DNA in aqueous solutions using a combination of spectroscopic, calorimetric and simulation methods. We found that both urea and TMG dehydrate DNA and shift the conformational equilibrium from B- to A-DNA form, despite different solvation properties. The isolated vibrational spectra of osmolytes and analysis of preferential accumulation indicate a lack of direct specific interaction with DNA in ternary solutions. Besides the influence of TMG and urea on DNA hydration, we studied and analyzed the orientational and spatial distribution of osmolytes around DNA. Analysis of hydrogen bonds and theoretical calculations of interactions with native and denatured DNA show strong negative interactions with bases of dissociated DNA: while TMG preferentially interacts with guanine, urea interacts equally strongly with all bases. This high affinity of both TMG and urea towards DNA bases appears to be the cause of their denaturing properties.

1 Introduction

The ability to adjust both the osmotic pressure and the stability of biomacromolecules to changing environmental conditions is crucial to the survival of many living organisms. It can be achieved by intracellular accumulation of osmolytes – small organic molecules are known to perturb the folding equilibrium of proteins and nucleic acids. Based on chemical and structural properties, naturally occurring osmolytes can be divided into three groups: (i) polyols, e.g. glycerol or mannitol; (ii) amino acids and their derivatives, e.g. taurine or β-alanine; and (iii) urea and methylamines, e.g. TMAO, TMG(65; 30; 64; 66; 40). Most commonly, though, osmolytes are divided according to their impact on protein stability, with some shifting the folding equilibrium toward the native form (stabilizing, e.g. betaine) and some toward the unfolded form (destabilizing, e.g. urea). While a number of theories exist to explain the stabilizing and destabilizing effects of osmolytes on proteins, these are usually not directly transferable to the case of nucleic acids, as highlighted by the fact that some protein-stabilizing osmolytes destabilize the double helix of DNA. It therefore remains unclear whether the folding equilibrium of DNA is perturbed by direct interactions between solvent and the DNA molecule, or indirectly, by osmolyte-water interactions that modify the properties of the solvent(11; 9; 42; 48; 7; 25; 47; 31). Yet, knowledge of the mechanisms governing the effect of solvent on DNA stability is of great practical importance due to applications in genetic engineering and biotechnology such as enhancement of GC-rich template amplification or prediction of stability of secondary DNA structures across a range of experimental conditions.

DNA exhibits significant conformational variability, and among the major factors determining the relative stability of individual secondary structures are the interactions between the solvent and the DNA molecule. These interactions also contribute to the variability of DNA function, including the binding of various ligands(56; 62; 49; 14; 32; 38). Of particular interest is the tendency to change the conformation from A-DNA to B-DNA depending on water activity(50; 19). Studies using infrared and UV spectroscopy have shown that full hydration of DNA molecule is essential to maintain the integral structure of the DNA, and that decreasing the relative humidity results in improper alignment of base pairs in the helix(17). In addition, the tendency to form A- or B-DNA is highly sequence-dependent, suggesting that the final secondary structure is dictated by an intricate interplay of subtle

contributions(27; 61; 29; 39).

While water is key to the stabilization of biologically active DNA structures, osmolyte molecules are known to disturb spatial arrangement and the interaction patterns of water molecules, causing water to manifest altered physicochemical properties – such as lower activity – than in its pure state. In consequence, both decreasing the relative humidity during crystallographic experiments(19; 2; 44) and addition of organic cosolvent or salt(26; 45; 41; 20) were similarly found to preferentially stabilize A-DNA.

To investigate the molecular mechanism underlying this conformational shift, in this study we chose representatives of two groups of osmolytes believed to modulate the stability of biomacromolecules in solution in different ways. TMG was selected from the group of peptide stabilizing osmolytes, which are mostly excluded from the peptide surface, therefore interacting through water molecules. Urea was chosen as a model of the peptide denaturant, that mostly acts by forming direct interactions with the biopolymer. These two modes of action – by affecting of water having changed properties due to presence of the solute and by direct interactions with the solute, also termed as "indirect" and "direct" – are an important distinguishing feature in the context of the dominant theory of osmolytic influence on peptides in solution(11; 9; 42; 48; 7; 25; 47; 31). The mentioned distinction entails also thermodynamic consequences (primarily of the entropy nature), which are often considered as the main factor controlling the folding/unfolding equilibrium of peptides(13; 22; 3; 52). However, it is known that both TMG and urea exert a similar effect on DNA, reducing its stability and accelerating the denaturation of the double helix, hinting at a more intricate mechanism at play(39; 5; 4; 53; 46; 54).

This work aims to explain this destabilizing effect by establishing a connection between the structural, thermodynamic and spectroscopic properties of DNA and the molecular interactions of TMG and urea with DNA in aqueous solutions. Well-known, and easy accessible Calf Thymus DNA (ctDNA) was chosen for experimental studies. FTIR spectroscopy and calorimetry, as well as molecular dynamics simulations, were utilized to obtain a complementary description of osmolyte-induced DNA denaturation. In particular, FTIR vibrational spectra along with the simulational analysis of geometric determinants of DNA allowed us to establish how osmolytes affected the secondary structure of DNA. We have shown in the Supplementary Information section S.1 that addition of phosphate buffer and sodium chloride exerts a strong effect on ctDNA. The presence of the buffer influences the melting temperature much strongly than osmolytes studied in this work. Furthermore, the shape of the thermogram of ctDNA denaturation in the buffer is changed significantly relative to the thermograms in the water and in the buffer solution, pointing to a different mechanism of DNA influence. To avoid complications in this already complex system and avoid darkening the image of interactions and influence of studied osmolytes on DNA, we did not use a buffer in our investigations.

2 Experimental and Theoretical Methods

2.1 Materials

Calf thymus double-stranded DNA (ctDNA, Sigma), N,N,N-trimethylglycine (TMG, betaine glycine, 99%. Fluka), urea (98%, Sigma), sodium chloride (NaCl ≥ 99%, POCh) and tetrabutylammonium chloride (TBACl ≥ 99%, Sigma) were used as supplied. The deionized water of κ=0.08 μS·cm^{-1} was used for the preparation of all solutions and for all measurements. Studies described in this paper were conducted in the aqueous environment without a buffer, which is justified in the Supplementary Information section S.1

2.2 FTIR spectroscopy.

Solutions of urea were prepared in deionized water in the range of 0.0 - 7.0 mol·dm^{-3} and were later used to dissolve appropriate weighted amounts of ctDNA to obtain a concentration of 80 mg·mL^{-1}. Similarly, solutions of TMG were prepared in deionized water in the range of 0.0 - 3.5 mol·dm^{-3} and were later used to dissolve ctDNA to its final concentration of 80 mg·mL^{-1}. The concentration of ctDNA was the lowest possible concentration allowing to obtain signal intensity sufficient for its further evaluation and interpretation. At the same time concentration of both osmolytes covers their solubility range in water. ctDNA solutions were incubated for 24 hours at 4°C to allow for full dissolution of

2

ctDNA. All solutions have been prepared by weight and their densities were measured using Anton Paar DMA 5000 densitometer at $25.000 \pm 0.001°C$.

FTIR spectra of water solutions of ctDNA, osmolytes, and mixtures were recorded on a Nicolet 8700 spectrometer (Thermo Electron Co.). For each spectrum, 256 or 512 scans were made with a selected resolution of 2 cm^{-1} within the range of 550–4500 cm^{-1}. The attenuated total reflection (ATR) technique was applied for measurements of DNA and DNA-osmolyte solutions. The Golden Gate ATR accessory (Specac Inc.) was used, equipped with a single-reflection diamond crystal. During measurements, the temperature was kept at $25 \pm 0.1°C$ using an electronic temperature controller (Specac Inc.). The spectrometer's EverGlo source was in "turbo" mode during measurements. The spectrometer and ATR accessory were purged with dry nitrogen to minimize water-vapor contamination of the spectra. All ATR spectra were water and vapor-subtracted, ATR-corrected using an advanced ATR correction algorithm (part of the OMNIC software) and smoothed with a 9–13-point Savitzky-Golay filter.

Isolation of the spectra of ctDNA affected by osmolytes and spectra of osmolytes affected by ctDNA was carried out analogously to the procedure described in detail in references(10; 12; 11). All affected spectra were normalized, which means that analyzed bands were reduced to a surface area equal to 1. Normalization was necessary due to differences in concentrations of studied individuals within one measurement series. This allowed to analyze the differences in the shape and position of bands resulted from the DNA-osmolyte interaction. All calculations were performed in Matlab 2010 environment (MathWorks. Inc.) using custom scripts and a commercially available script for spectra isolation algorithm (part of Factor Analysis Toolbox, Applied Chemometrics. Inc.), based on the published Malinowski's algorithm(34; 35).

2.3   Differential Scanning Calorimetry (DSC)

Solutions of urea were prepared in deionized water in the concentration range of 0.000–0.084 mol·dm^{-3} and were later used to dissolve appropriate weighted amounts of ctDNA to obtain a concentration of 1 mg·mL^{-1}. Solutions of TMG were prepared in deionized water in the concentration range of 0.000–0.042 mol·dm^{-3}. They were later used to dissolve ctDNA to its final concentration of 1 mg·mL^{-1}. The concentration of osmolytes was prepared so as to obtain an appropriate ratio of the number of test compound molecules to the number of phosphate groups in the ctDNA solution after titration. These proportions were selected to keep the experimental conditions of FTIR spectroscopy tests. The concentration of 1 mg·mL^{-1} of ctDNA was eighty times smaller than the concentration used in the FTIR spectroscopy experiments, however it was the highest concentration that could be applied using DSC apparatus. Keeping in mind the difference in concentrations in both types of experiments, for the DSC measurements osmolytes concentration was lowered accordingly (eighty times). ctDNA solutions were incubated for 24 hours at 4°C to dissolve the DNA. All solutions have been prepared by weight.

Calorimetric measurements were carried out with use of the Nano-Differential Scanning Calorimeter III (TA Instruments). It was equipped with two capillary cells with the capacity of 0.33 mL. The reference cell contained an aqueous solution of osmolyte, and the reaction cell contained ctDNA in an aqueous solution of osmolyte. Scanning was carried out in the temperature range of 10–100°C at the rate of 1°C per minute, at a constant pressure of 3 atmospheres. Data was collected using Nano DSC Run 4.0 (TA Instruments) and analyzed with NanoAnalyze 2.1 (TA Instruments). Calorimetric measurements yielded melting curves of ctDNA in water-osmolyte mixtures. The average ctDNA melting temperature was determined as a location of center of gravity of surface area under thermogram curve.

2.4   Isothermal Titration Calorimetry (ITC)

Solutions of urea and TMG were prepared in deionized water. The concentration of osmolytes was prepared so as to obtain an appropriate ratio of the number of test compound molecules to the number of phosphate groups in the ctDNA solution after titration. These proportions were selected to keep the experimental conditions of FTIR spectroscopy tests. Solutions of ctDNA were prepared in deionized water to obtain a concentration of 1 mg·mL^{-1}. DNA solutions were incubated for 24 hours at 4°C to dissolve the DNA. All solutions have been prepared by weight. Solutions of auxiliary compounds, NaCl and TBACl, were prepared in deionized water so that the number of substance molecules in a solution corresponded to the number of phosphate groups of ctDNA in the sample solution.

The calorimetric measurement was carried out with use of the Nano-Isothermal Titration Calorimeter III (Calorimetry Sciences Corp.). It was equipped with two measuring cells with the capacity of 1 mL. The reference cell contained pure water, while the reaction cell contained an aqueous solution of the tested substance. Osmolyte solution was titrated using a precise burette with a capacity of 250 μL. Measurements were carried out at a constant temperature of 25°C. Solution aliquots were automatically dosed with a capacity of 10 μL every 300 seconds. The reaction mixture was stirred at 250 rpm. Data was collected using Nano DSC Run 4.0 (TA Instruments) and analyzed with NanoAnalyze 2.1 (TA Instruments). The pH of all solutions was controlled by a pH-meter from Schott, equipped with a glass microelectrode.

An ITC calorimeter measures the global thermal effect which accompanies the mixing of solutions of two reagents: titrant and analyte. The global thermal effect consists of a number of different contributions. In addition to enthalpy changes associated with 'breaking' of old and 'formation' of new bonds, the global effect is also influenced by dilution enthalpy and enthalpy of mixing, the latter dependent on differences in pH, concentration, and temperature between both solutions. Accordingly, the heat of examined processes has been estimated on a basis of series of titration experiments described in SI section S.2.

2.5   Molecular systems and simulations procedure

Initial coordinates of a 16-bp long double-stranded B-DNA helix with 5'-AGTCTAACTTGCATCT-3' sequence were generated using the X3DNA program(15). In all systems, DNA was solvated with TIP3P water molecules(28) and a proper number of osmolyte molecules in a dodecahedral 6.62 nm × 6.62 nm × 6.62 nm box. 14 different solutions were simulated: the osmolyte-free system, for TMG, the concentrations ranged from 1.0 to 3.5 M every 0.5 M; for urea, an additional concentration of 5.0 M was also used (see Table S1 in SI for detailed compositions of the individual systems). 30 sodium ions were added to neutralize the charge of the DNA backbone. The CHARMM27 force field(18) was used for DNA and ions. The force field parameters for urea were taken from the CHARMM General Force Field (CGenFF) (60) and for betaine we used the previously validated parameter set obtained by analogy from the CHARMM parameters for phospholipid headgroups (trimethylammonium group from phosphatidylcholine; carboxylic group from phosphatidylserine)(1).

All MD simulations were ran using Gromacs 4.6.5(24) in the NPT ensemble with the reference temperature and pressure of 300 K and 1 bar, respectively. Periodic boundary conditions were applied in 3D, and electrostatic interactions were calculated using the particle mesh Ewald (PME) method with a real-space cutoff of 1 nm and a Fourier grid spacing of 0.1 nm. A cut-off of 1 nm was used for Lennard-Jones interactions. Bond lengths were constrained using P-LINCS(23) for DNA and osmolytes and SETTLE(37) for water. The equations of motion were integrated using the leap-frog algorithm with a 2 fs time step. The total simulation time for each systems was 1 μs.

To prepare denatured states of DNA for all systems, the two strands of DNA were forced to dissociate over 500 ns by applying an external harmonic potential (with the force constant of 2092 kcal/(mol·nm²)) to the collective variable defined as the minimal distance between all phosphate groups from two individual strands (see Equ.1 in SI section S.3). A fully dissociated state was achieved when the minimal distance exceeded value of 2 nm, after which the systems were subject to 1 μs equilibrium MD simulation with the condition MinDist ≥ 2 nm. This procedure was carried out using the PLUMED 2.0 plugin(57) coupled to Gromacs 4.6.5.

The GC content in the model DNA molecule (without taking into account 3' and 5' terminal bases) corresponds to the mean GC content of ctDNA (40% GC, 60% AT). The terminal bases have been omitted from our analyses because of the unrealistic effects of solvation on the fraying ends of the double helix.

3   Results and Discussion

3.1   ctDNA structure affected by osmolytes

By analyzing the perturbed IR spectra of DNA in different solvent conditions, one can observe changes in frequencies and intensities of specific vibrational modes in the DNA molecule, obtaining valuable information on the strength and type of solute-solvent interactions molecules, as well as changes in the

local geometry of the DNA helix. Within the spectral region between 1270 and 900 cm^{-1}, we analyzed four bands characteristic for dsDNA centered at 1222, 1086, 1053 and 970 cm^{-1}, corresponding to antisymmetric PO2^{-} stretching, symmetric PO2^{-} stretching and sugar bond C-O stretching as well as C-C stretching vibrations in the DNA backbone, respectively. Series of isolated and normalized spectra of ctDNA are presented in Fig. 1.

The band at 1222 cm^{-1} is the main marker of the B form of DNA. In the highest concentration of TMG used in this study (3.5 M), the band is shifted by about 8 cm^{-1} toward higher wavenumbers. TMG also affects band intensity, with the nonlinear dependence on osmolyte concentration (inset in Fig. 1A) indicating that the mechanism of TMG impact on ctDNA is complex and could be divided into concentration-dependent stages. Similarly, in urea solutions, this band broadens and shifts towards higher frequencies (about 5 cm^{-1} for the highest concentration of urea) compared to ctDNA in a pure aqueous solution. While the presence of urea also changes the intensity of absorption of the 1222 cm^{-1} band in a non-linear fashion, the shift is monotonous and saturates at high concentration.

Quite different trends are found for the bands at 1086 cm^{-1} and 1053 cm^{-1}, where increasing the concentration of TMG results in a linear decrease of band intensity, additionally shifting the band at 1053 cm^{-1} towards higher wavenumbers. The addition of urea only slightly affects the intensity of bands in the 1150 - 980 cm^{-1} region, indicating that this region is almost insensitive to the presence of urea in solution. Despite the minor observable changes, bands at 1086 and 1053 cm^{-1} are the least altered by the presence of osmolytes compared to the other two regions.
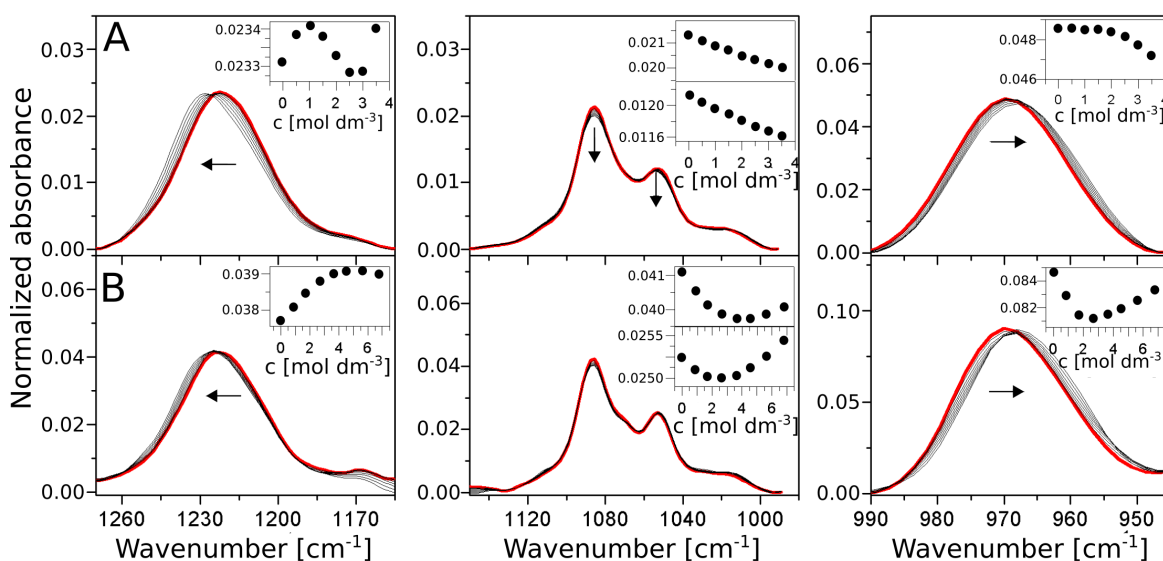

Figure 1: Infrared absorption spectra of calf thymus DNA in aqueous solution in the presence of (A) TMG (12) and (B) urea in three selected regions (without osmolyte - red line, with osmolyte - black line). The insert shows the band intensity as a function of osmolyte concentration.

Finally, under the influence of TMG in DNA solution both intensity and breadth of the 970 cm^{-1} band decrease, with the peak shifting towards lower wavenumbers. Urea shifts the maximum in a similar manner but the absorption intensity first decreases and then increases after reaching a certain cosolvent concentration.

According to Falk(17), two effects might be observed during the hydration of DNA: narrowing of selected bands in studied region and change in their frequency. Typically, increasing humidity of DNA shifts the bands at 1222, 1086 and 1053 cm^{-1} towards lower wavenumbers, while shifting the band at 970 cm^{-1} to higher wavenumbers. Therefore, the broadening of bands and the specific peak shifting pattern observed in our case can be explained as dehydration of DNA. Consequently, it can be assumed that increasing the osmolyte concentration causes progressive dehydration of DNA. Moreover, conformation of DNA is known to depend on the relative humidity of DNA(58). While A-DNA conformation prevails in solution at a relative humidity above 75%, the formation of B-DNA requires a relative humidity of 92%. This strongly suggests that the addition of osmolytes to solution

5

causes dehydration of DNA, resulting in a transition from the B to A form. In extreme cases, the macromolecule might undergo full denaturation.

3.2   Osmolyte - ctDNA affected spectra

While discussing the impact of osmolytes on DNA it is necessary to clearly distinguish between variation of parameters of oscillation band in DNA spectrum and participation of DNA structure perturbation (expressed in %) in the whole macromolecule, both due to osmolyte presence in the system. The degree of variations of band parameters is more important in aspect of intermolecular interactions. That indicates direct, often specific DNA-osmolyte interaction. While values specifying DNA perturbation (%) may be a valuable source of additional information resulted from indirect interactions (e.g. through water) or an effect of change of molecular surrounding of affected DNA molecule.
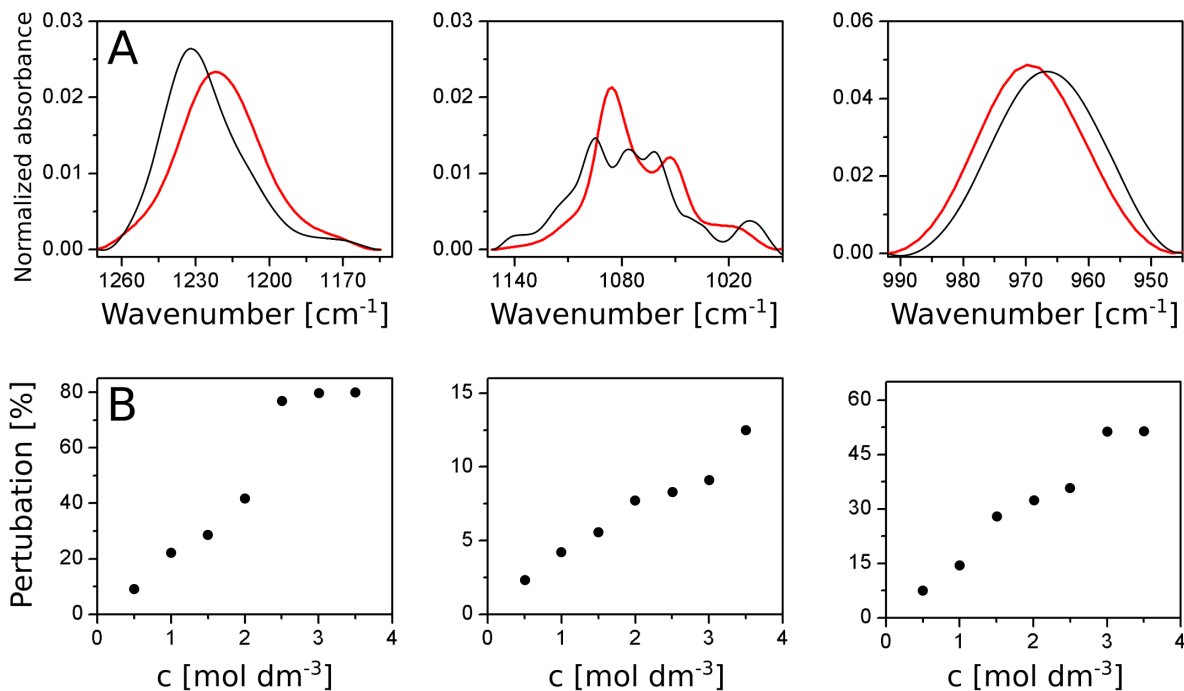

Figure 2: (A) Spectra of ctDNA in water (solid red line), and corresponding affected spectra of ctDNA by TMG (solid black line). All spectra are divided into three specific spectral regions. (B) Dependence of percentage of ctDNA perturbation on concentration of TMG calculated for corresponding regions of spectra.

TMG causes progressive increase of intensity of ctDNA affected spectrum in the region of band at 1222 cm^{-1} and shifts it to higher wavenumbers (Fig. 2). Significant shift of this band to 1232 cm^{-1} can be observed while applying the highest concentration of mentioned osmolyte. This shift can be explained by reduced (by presence of osmolyte) activity of water which leads to both, reduction of interactions of perturbed water molecules with phosphate groups and partial transition from B to A form of DNA(6). The percentage of perturbed form of ctDNA reaches a value of 80%. Dependence of perturbation on osmolyte concentration (Fig. 2B) is complex and indicates that TMG rapidly alters mentioned region of spectrum associated with specific components of DNA structure. Analyzing changes in value of perturbation parameter, three distinct stages of influence of TMG on ctDNA dependent on concentration of osmolyte might be observed. The ctDNA affected spectrum in the region of band at 1222 cm^{-1} shifts to higher wavenumbers when influenced by urea (Fig. 3A). Broadening of this band is also noticeable. Analyzing the changes which occur in percentage of perturbation of ctDNA structure with increasing urea concentration, three-step dependence can be observed, similarly to TMG. However, urea induces very small changes in ctDNA structure - the highest analyzed concentration of this osmolyte creates only a 15.4% of perturbed structure of ctDNA (Fig. 3B). Summing up, urea exhibits less extensive indirect influence on the phosphate groups than TMG.
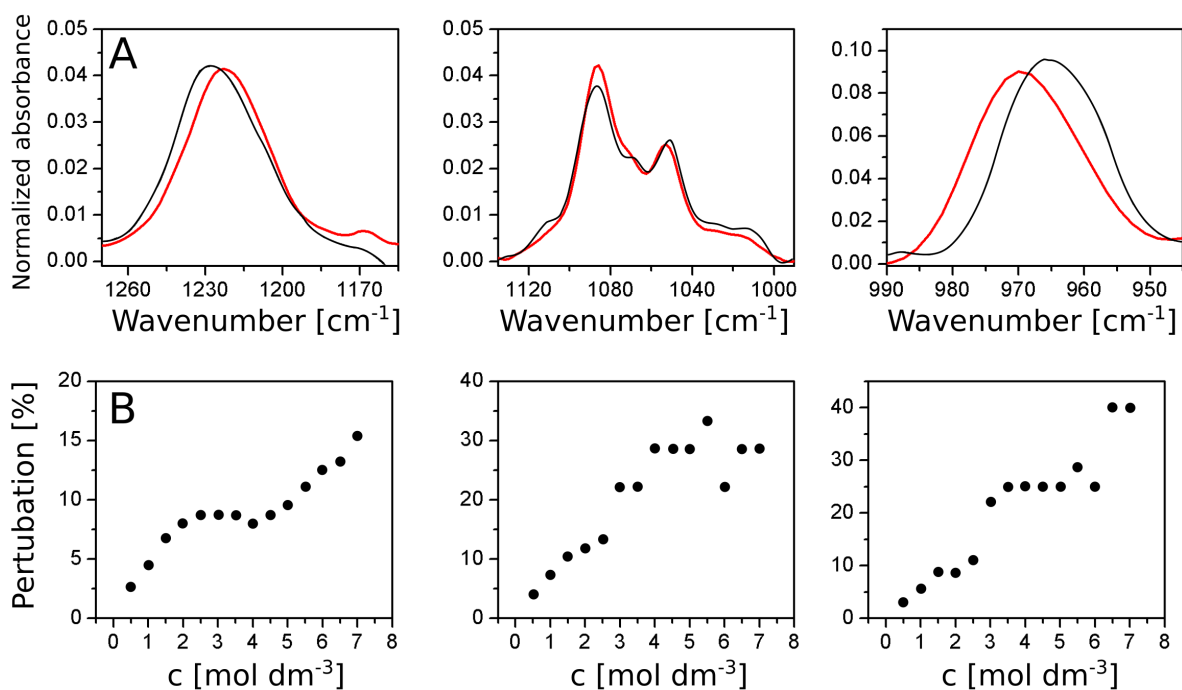
Figure 3: (A) Spectra of ctDNA in water (solid red line) and corresponding affected spectra of ctDNA by urea (solid black line). All spectra are divided into three specific spectral regions. (B) Dependence of percentage of perturbation on concentration of urea calculated for corresponding regions of spectra.

The second examined region of ctDNA spectrum includes two bands: 1086 and 1053 cm^{-1} associated with two different structures of DNA. Therefore, it is necessary to take into account that perturbations appeared in resulting spectra may have various origins. The percentage of perturbed ctDNA structure within this region increases stepwise with increasing concentration of TMG and reaches value of 12.5%. The slope of this dependence is low and indicates small changes in ctDNA structure due to increasing osmolyte concentration (Fig. 2B). However, modification of the structure is very explicit - contour of affected band is altered if compare to pure ctDNA solution (Fig. 2A). The ctDNA affected spectra obtained within the same region for urea are similar to spectra of ctDNA without osmolyte in solution (Fig. 3A). The main difference appears in band at 1086 cm^{-1} and this is decrease of its intensity. Urea induces slight changes of two analyzed bands parameters and thus exhibits very small impact on phosphate groups and C-O bonds of deoxyribose residues. Percentage of perturbed structure of ctDNA reaches a value of 28.6% for the highest analyzed concentration of urea. Changes in structure occur gradually with increasing osmolyte concentration (Fig 3B). The band at 970 cm^{-1} in third analyzed region is a marker of B-DNA form as same as band at 1222 cm^{-1}. TMG shifts 970 cm^{-1} band of ctDNA to lower wavenumbers and slightly reduces its intensity (Fig. 2A). For the highest TMG concentration share of perturbed structure of ctDNA was determined to be equal 51.3%. Similarly as in other regions, process of interaction of this osmolyte with ctDNA is stepwise (Fig. 2B). Urea broadens the band at 970 cm^{-1} and shifts it to lower wavenumbers (Fig. 3A). This change of affected band parameters is larger than for TMG, thus impact of urea on ctDNA structure within this region is stronger than impact of TMG. For the highest analyzed concentration of urea (7 mol·dm^{-3}) 40% of perturbed structure of ctDNA can be observed (Fig. 3B).

3.3 CtDNA - osmolyte affected spectra

Determination of N parameter value allowed to obtain an affected spectrum of osmolyte perturbed by ctDNA (Fig. 4). For the TMG this value is significantly greater than for urea (Table 1).

In affected spectrum of osmolyte a spectral range between 4000 and 2500 cm^{-1} corresponding to stretching vibrations of C-H and N-H bonds was excluded from analysis. In this range very intensive band corresponding to stretching vibrations of water also occurs and should be subtracted. However, taking into account participation of water affected by presence of osmolyte and ctDNA in solution,

7

Table 1: Values of chemometrically determined N parameter for osmolytes perturbed by ctDNA in solution.

Osmolyte	N^a
TMG	6.4
Urea	1.0

a - number of affected molecules of osmolyte equal to number moles of osmolyte affected by one nucleotide

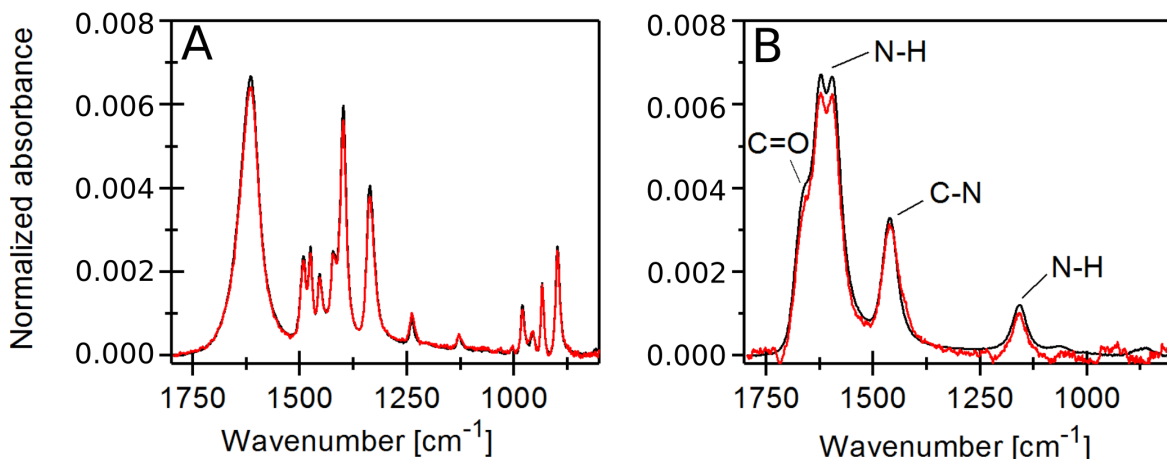this procedure cannot be carried out quantitatively.

Figure 4: Comparison of osmolyte in water spectrum (black line) and 'affected spectrum' of osmolyte by ctDNA (red line) for (A) TMG and (B) urea(43).

Determined affected spectra of TMG (Fig. 4A) and urea (Fig. 4B) in presented region are almost identical to spectra of corresponding osmolytes in water. There are no shifts or significant changes in 'affected spectra' when compared to 'not-affected spectra'. That suggests a lack of direct, specific interactions between osmolytes and ctDNA or that interactions of osmolytes with the DNA resemble interactions with water molecules. The last statement may have a special application for urea, as the results of MD simulation (presented in the following chapters) do not allow neglecting the direct interaction of urea with DNA molecule.

3.4 ctDNA thermal stability affected by osmolytes

Thermograms obtained using DSC calorimetry were used to determine a melting temperature (T_m) of ctDNA in presence of TMG or urea in solution. It is known that glycine and its N-methyl derivatives induce decrease of melting temperature of DNA and thereby reduce its stability(48; 7; 46; 54). According to Barone(7) the value of T_m of ctDNA is 67.2°C and upon increasing the TMG concentration, T_m decreases almost linearly. Such behavior was not observed in our experiments, were in the presence of TMG non-linear dependence of melting temperature on osmolyte concentration might be observed (Fig.5, Table2). Moreover, presence of minimum of melting temperature is noticeable. That indicates increase of ctDNA thermal stability in osmolyte concentration higher than 0.032 mol·dm^{-3}. Such observation might argue for appearance of stabilizing interaction in DNA-water-osmolyte system above certain TMG concentration. Observed discrepancies between our results and these reported in the literature(7) arise from lack off buffer and sodium chloride in our experiments. Specific pattern of dependence of ctDNA melting temperature vs. osmolyte concentration observed by us can be explained later based on the molecular dynamic results about arrangement of osmolyte molecules relative to the DNA surface. Similar conclusions can be drawn for urea, with the difference that stabilizing interaction with ctDNA appears at higher concentration of 0.060 mol·dm^{-3}. It should be noted that for both osmolytes concentration range used in the DSC experiments the possible osmolyte self-association is completely negligible(16; 55; 21; 63).
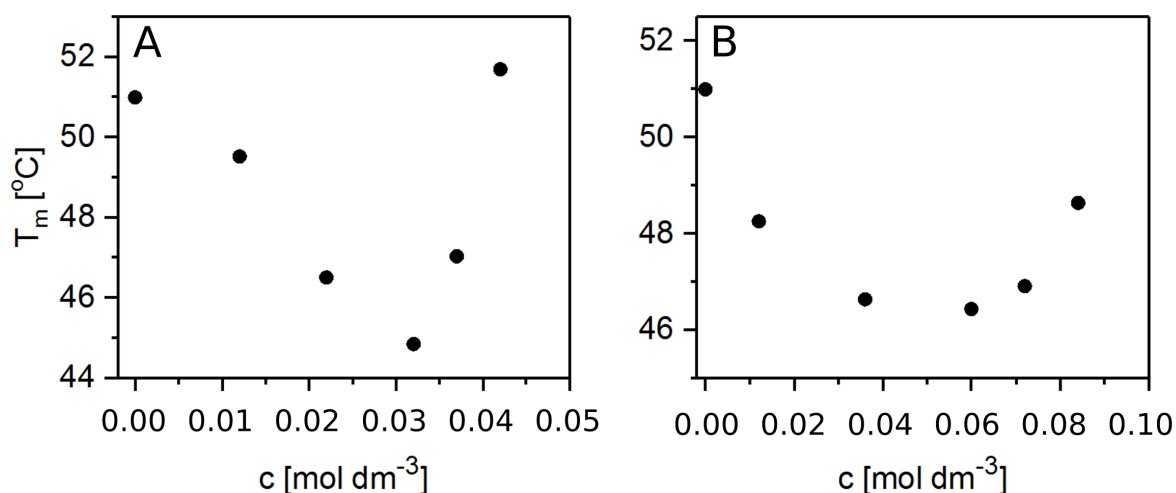
Figure 5: Dependence of melting temperature of ctDNA on concentration of TMG (A) and urea (B).

Table 2: Dependence of ctDNA melting temperature on osmolytes concentration.

	c^a $mol \cdot dm^{-3}$	T_m^b $°C$	ΔT_m^c $°C$
DNA	0	50.99	
TMG	0.012	49.51	-1.48
	0.022	46.50	-4.49
	0.032	44.84	-6.15
	0.037	47.03	-3.96
	0.042	51.69	+0.70
Urea	0.012	48.25	-2.74
	0.036	46.63	-4.36
	0.060	46.43	-4.56
	0.072	46.90	-4.09
	0.084	48.68	-2.36

a - osmolyte concentration
b - ctDNA melting temperature
c - change of ctDNA melting temperature in presence
of osmolyte in solution compared to ctDNA solution
without osmolytes

3.5 ctDNA interaction with osmolytes

Series of ITC thermograms (see SI section S.2) indicate a lack of direct specific ctDNA interaction with osmolytes. Observed heat effects accompanying series of injections of osmolyte solution to ctDNA solution are almost invariant what excludes formation of complexes and any other specific interactions. Due to non-typical character of the ITC thermograms they have been utilized only for determining a value of global heat effects of osmolyte interaction with sodium ions or ctDNA. All values of enthalpy as a function of molar ratios (osmolyte to ctDNA base pairs or sodium ions) were extrapolated to zero value i.e. infinite dilution of solute conditions. ctDNA titration by TMG or urea is accompanied by slight exothermic effect. Determined global effect consists of a number of sub-effects: (a) effect of partial destruction of hydration shell of osmolyte and sodium salt of ctDNA (endothermic effect), (b) effect of electrostatic interactions, molecular contacts and possible specific interactions between osmolyte and NaDNA (exothermic effect), (c) effect of reconstruction of hydration shell of interacting molecules (exothermic effect) and (d) effect of change of NaDNA internal energy due to change of ctDNA structure, change of energy of hydrogen bonds between complementary bases, change of energy of stacking interactions between bases and energetic effect accompanying a possible displacement of sodium ion in solvation shell of phosphate group of ctDNA.

Table 3: Enthalpy effects characterizing osmolyte interaction with sodium ions and sodium salt of ctDNA.

	ΔH^a_{NaDNA}	U^b_{95}	$\Delta H^c_{Na^+}$	U^b_{95}
	kJ/mol		kJ/mol	
TMG	-2.90	0.37	0.13	0.30
Urea	-2.12	0.22	-2.51	0.39

a - enthalpy of interaction between sodium salt of ctDNA (NaDNA) and osmolyte, extrapolated to infinite dilution of osmolyte
b - expanded uncertainty for confidence level of 95%
c - enthalpy of interaction between sodium cations and osmolyte, extrapolated to infinite dilution of osmolyte

Interactions of Na^+ with osmolytes were also analyzed. Determination of enthalpy of these interactions was crucial for better understanding of intermolecular interactions in analyzed ctDNA solutions. In case of TMG suppression of energetic effect of sodium ions interaction with water by thermal effect of newly created interactions of this cations with osmolyte might be observed. This happens in contrary to expected increase of donor ability of glycine derivatives with increasing number of methyl groups. Therefore, increasing steric hindrance of methyl groups of TMG coordinating to Na^+ ions appears to be a determinant of observed effect. In contrast, when urea was added to water solution containing sodium ions a small exothermic effect was observed. On the base of this result it can be concluded that interaction of sodium ions with water molecules is slightly weaker than arising interaction of this cations and urea.

3.6 Preference of water and osmolytes to ctDNA in the MD simulations

To determined the density changes of osmolyte and water molecules around DNA molecule, first we calculated solvent density function (SDF). SDF was calculated for the center of mass of osmolyte molecules and water molecules relative to the surface of DNA. Due to the fact that the DNA molecule does not have spherical symmetry, we normalized raw pair distribution data by the factor calculated as the solvent-accessible volume of the shell based on the methodology by Daggett et al.(8; 51) Additionally, in order to omit the edge effects, the calculations did not take into account the terminal base pairs.

SDF's in Fig. 6A and Fig. 6B shows that TMG and urea molecules close to DNA surface have an increased density relative to the bulk density (red an blue lines). Urea density is definitely higher than betaine, however for both osmolytes densities are dependent on the concentration of osmolytes and decrease with increasing concentration. Solvation shell formed by TMG molecules is wider and shifted to longer distances than for urea and with the magnitude of accumulation similar to the water accumulation. An additional peak for betaine above 0.4 nm suggests the indirect interaction of betaine with DNA.

SDF's in Fig. 6A and Fig. 6B also shows, that TMG does not change the distribution of water molecule close to the surface of the DNA (green lines). Only solutions of urea have a slight influence on the distribution of water molecule around DNA surface. Even in low concentrations of urea, the density of water is reduced relative to the bulk water solution and further increasing the concentration of urea reduced hydration shell.

Next, we sought to identify the molecular determinants of the experimentally observed effect of osmolytes on the denaturation of DNA. Since, it is commonly believed that the stabilizing or destabilizing effect of osmolytes on the DNA structure results from their attractive (favorable) or repulsive (unfavorable) interactions with the DNA, we examined whether urea and betaine are preferentially excluded from or accumulated at the DNA surface, and how these preferential interactions vary with solution concentration. For this purpose, we calculated the preferential interaction coefficient Γ, which definition is in SI section S.4.

Fig. 6C shows, that negative values of Γ in the first solvation sphere (¡0.4 nm) obtained for betaine indicate that the osmolyte molecules are effectively repulsed by the DNA surface, with the exclusion being most pronounced in the immediate vicinity of the DNA ($\Gamma = -25$ for r = 0.34 nm at 3.5 M). It
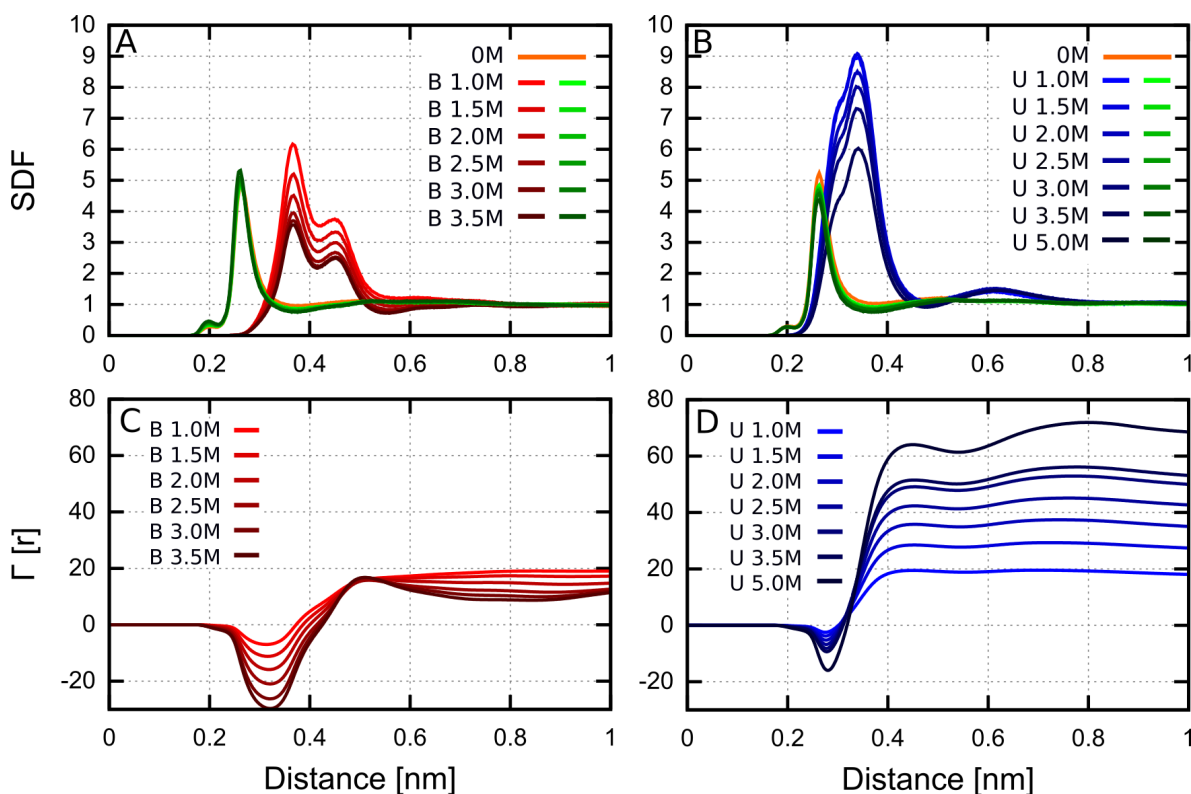
Figure 6: A,B The solvent density function for the center of mass of TMG (red lines in A), urea (blue lines in B), water molecules in a solution of osmolyte (green lines in) and water molecules in solution without osmolyte (orange line) to DNA surface. Color tone according to the concentration of osmolyte. C) D) Preferential interaction coefficient (Γ) between the osmolyte and DNA, calculated for all betaine and urea solutions, as a function of the separation distance from the DNA surface. Decreasing values of Γ show that betaine is more strongly excluded from and urea more accumulated at the DNA surface with increasing concentration.

can be also seen that the number of betaine molecules excluded from the DNA surface increases with concentration. For distances greater than 0.4 nm there is a small aggregation of betaine associated with the second solvation sphere.

For all the urea solutions in Fig. 6D, it can be seen that Γ is positive in almost the entire distance range considered, indicating accumulation of the osmolyte at the DNA surface, which is typical for denaturants. Importantly, the amount of urea accumulated at the surface of DNA is markedly increased with increasing concentration, which is consistent with other studies on other nucleic acids(36).

3.7 Osmolytes interaction sites on DNA molecule in the MD simulations

To determine fragments of the DNA structure that are especially preferred by osmolytes we calculated the number of osmolyte molecules per nitrogenous base in native and dissociated state for whole DNA molecule, all nitrogenous bases, DNA backbone and individual nitrogenous bases. The total number of osmolyte molecules around the DNA is not the sum of the number of molecules around the individual DNA fragments, because the solvation spheres of individual DNA fragments can overlap.

Fig. 7 shows that the first solvation sphere of DNA in native and dissociated state contains more urea molecules per one nitrogenous base that TMG molecules despite the same solution concentration and different thicknesses of the first solvation sphere. This is also valid for the first solvation sphere of nitrogenous bases (RES) and the DNA backbone (BB) separately. Decomposition of preferences into nitrogenous bases and DNA backbone further shows that accumulation of the TMG and urea at the surface of DNA results mainly from a much larger number of osmolyte molecules around DNA backbone (75% of all molecules for TMG and 70% of all molecules for urea). Interestingly, during DNA
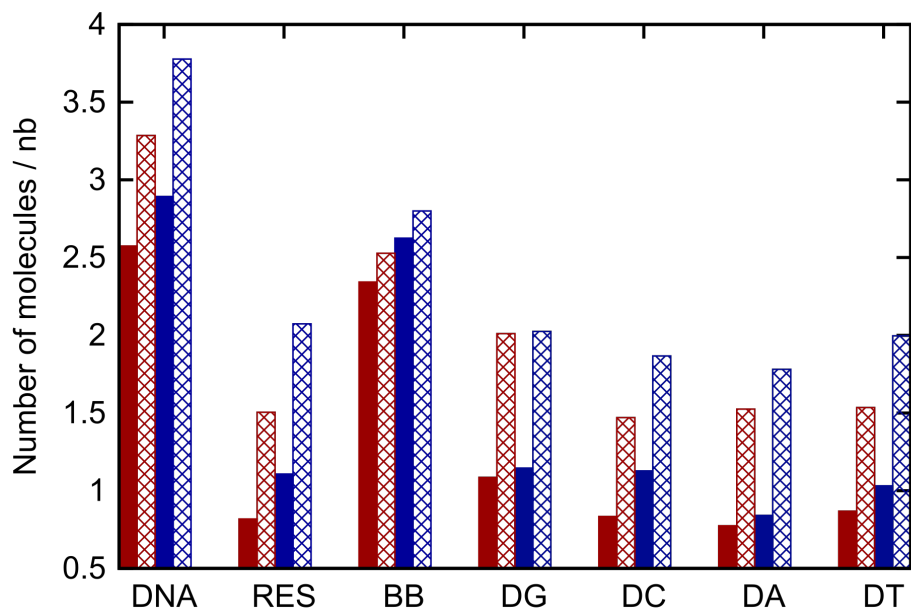
Figure 7: The number of TMG (red bars in A) and urea molecules (blue bars in B) per one nitrogenous base in the first solvation sphere in native (solid bars) and dissociated state (dashed bars) for whole DNA structure (DNA), nitrogenous bases (RES), DNA backbone (BB), guanine residue (DG), cytosine residue (DC), adenine residue (DA) and thymine residue (DT). Data only for 3.5 M TMG and 3.5 M urea solution. The value of the radius of first solvation sphere was chosen based on solvent density function in Fig. 6.

denaturation, the number of betaine and urea molecules in the first solvation sphere of nitrogenous bases increases by 185% and 175%, respectively. On the other hand, the increase in the number of osmolyte molecules for the DNA backbone is much smaller (6-8%).

Next, we checked the preference of osmolytes to specific nitrogenous bases. Fig. 7 shows the number of osmolyte molecules per one nitrogenous base (DG, DC, DA, and DT) in the first hydration sphere. In the native state, urea molecules show stronger accumulation for all type of nitrogenous bases than TMG molecules. Interestingly, for both osmolytes, we observed more molecules in the first solvation sphere of guanine-cytosine base pairs than around adenine-thymine base pairs. This is due to the fact that urea and TMG molecules exhibit less preference to adenine residues than to the guanine and cytosine residues. However, during denaturation, the largest increase in the number of betaine molecules is around guanine residues, whereas urea shows a uniform preference for nitrogenous bases. Summarizing, in the native and dissociated state urea shows preferences in the following order: DG ≈ DC > DT > DA, and TMG in the following order: DG > DT ≈ DC ≈ DA.

3.8   Impact of osmolytes on the distribution of water around DNA

It is suggested that osmolytes can change the hydration spheres of macromolecules by changing the water structure and hence the local density of water. However, the impact of osmolytes on the density of the water around DNA surface is not well known. Therefore, we determined the number of water molecules per one nitrogenous base in the first solvation sphere in native and dissociated state for whole DNA structure, nucleobase pairs and DNA backbone in native and dissociated state. In addition, we determined the percentage ratio between the observed and expected number of water molecules in the first solvation sphere.

Fig. 8A shows that in the aqueous solution without osmolyte (0M) DNA backbone is mostly responsible for hydration of whole DNA structure. After DNA denaturation, the number of water molecules per one nitrogenous base in the first solvation sphere for whole DNA structure increases, however, at the same time hydration of DNA backbone decreases in favor of nitrogen bases.

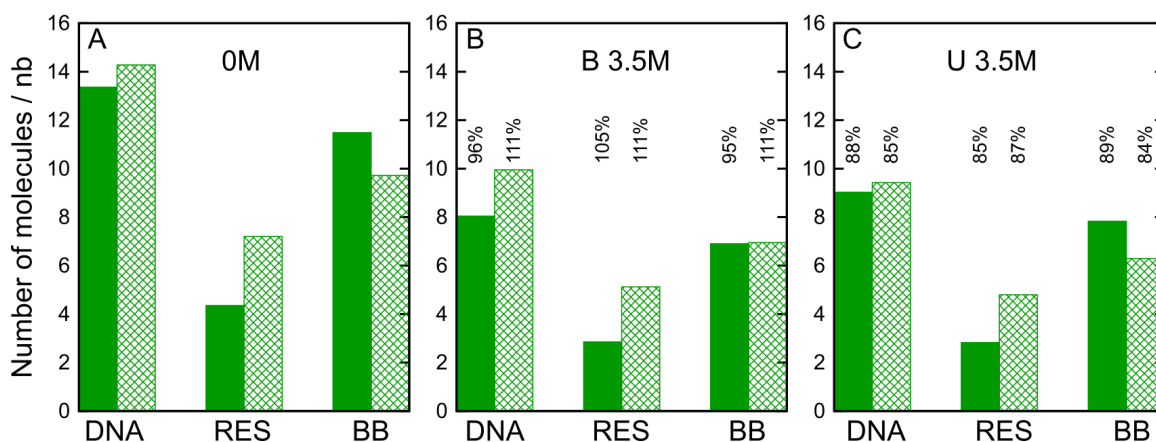The number of water molecules around whole DNA molecule after the addition of an osmolyte

Figure 8: The number of water molecules per one nitrogenous base in the first solvation sphere in native (solid bars) and dissociated state (dashed bars) for whole native DNA structure (DNA), nucleobase pairs (RES) and DNA backbone (BB). A) Data for the aqueous solution without osmolyte, B) 3.5 M TMG solution and C) 3.5 M urea solution. The percentage represents the ratio between the determined number of water molecules in the first hydration sphere to the expected number of water molecules in the first hydration sphere (see SI section S.5 for details). The radius of first hydration sphere was chosen based on solvent density function in the Fig. 6.

in native and dissociated state obviously decreases for both osmolytes, but a stronger reduction is observed for TMG solution (by 40%) than urea solution (by 30%). In the denatured state, the number of water molecules in the urea solution decreases, as in the aqueous solution without osmolyte. The betaine solution has a slightly different effect, in which hydration of the DNA backbone does not change and the number of water molecules for nitrogen bases normally increases.

We also observed the change in determined and expected number of water molecules in the first solvation sphere, which translates into a change in density of water that was not displaced by osmolyte (see SI section S.5 for details). It turns out that despite the decrease in the number of water molecules around the DNA in the betaine solution, the number of water molecules determined by us is close to the expected number, and for the denatured state much higher (111%). Urea, apart from the fact that it moves the water molecules away from the DNA, the number of water molecules determined by us is less than expected value by at least 10%. This indicates definitely worse solvation properties of water in a urea solution.

3.9   Arrangement and spatial distribution of osmolyte molecules relative to the surface of ctDNA

For a description of the orientation of the osmolyte molecules relative to the DNA surface, we determined the probability distribution of the angle between TMG and urea molecule axes and normal of DNA surface. The axis of TMG molecule was defined by the position of nitrogen atom and center of mass of oxygen atoms (see inset in Fig. 9A). For urea, the axis of molecule was defined by the oxygen atom and the center of mass of nitrogen atoms. Such a choice of molecule axes also almost perfectly describes vector of the dipole moments of osmolyte molecules.

Fig. 9A shows that TMG molecules are oriented towards the DNA surface by positively charged fragment (N$^+$ atom with methyl groups), while the arrangement of urea molecules is more complex. This result suggests that TMG molecules do not have much potential to interact specifically with DNA. Urea molecules mainly oriented towards DNA surface by amino groups, but significant fraction of molecules also have a parallel orientation with respect to DNA surface (high probability for angle values close to 90°). TMG molecules show a more monotonic angle distribution with respect to nucleobases than DNA backbone (dashed lines in Fig. 9), while in the case of urea molecules observed orientation around whole DNA surface results from the great arrangement to DNA backbone.

We also determined solvent density function for oxygen atoms of water molecules, nitrogen and oxygen atoms of osmolyte molecules shown in the Fig. 9 B and C. Nitrogen atoms of TMG and
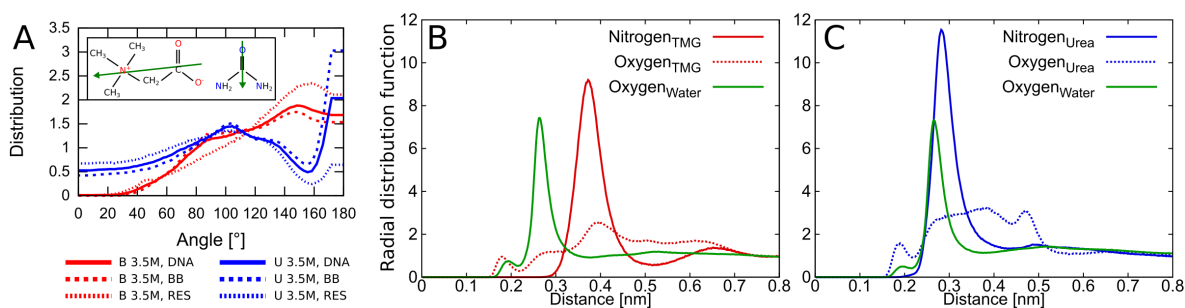
Figure 9: A Probability distribution of the angle between osmolyte molecules axes to the normal of the surface of DNA molecule (DNA, solid line), DNA backbone (BB, dashed line) and nucleobases (RES, dotted line). The inset shows atoms selected for the description of molecular axis: nitrogen and oxygen atoms for TMG molecules (red color) and oxygen and nitrogen atoms for urea molecules (blue color). Axis of the molecules is presented as a green vector. B,C solvent density function for nitrogen atoms of TMG (red solid line) and urea molecules (blue solid line), oxygen atoms of TMG (red dotted line) and urea molecules (blue dotted line) and oxygen atoms of water molecules (green lines).

urea molecules show increased density near the DNA surface, which confirms the interaction of these fragments of molecules with DNA. Theoretically, both osmolytes have the possibility to interact directly with DNA surface by oxygen atoms, however as shown by the SDFs in Fig. 9B and C definitely more urea molecules interact by oxygen atoms with DNA than TMG molecules. Additionally, oxygen atoms from urea show homogeneous density distribution in the range 0.25 nm to 0.5 nm. Only for a distance equal to 0.42 nm oxygen atoms from TMG molecules have increased density. This observation suggests that some fraction of TMG molecules are moved away from DNA surface and partially interacts with DNA through water molecules. These characteristic arrangements of osmolyte molecules may be responsible for the non-linear dependence of melting temperature in Fig. 5. Preferential orientation of both osmolytes by their positive poles of the dipolar moment (amino groups) to the phosphate groups of DNA (Fig. 10) results of electrostatic stabilization of the DNA helix.

To additionally confirm the described above preference and arrangement of osmolyte molecules around the DNA, we additionally calculated spatial distribution of osmolytes molecules around DNA molecule and the results are presented on two types of 2-dimensional density maps. First maps in Fig. 10 B and C show the density of osmolyte molecules along DR - distance from the axis of DNA helix and along the axis of DNA helix. Distance along the axis of DNA helix can be easily translated into position on the DNA sequence or number of the nucleobase. This means that this type of distribution shows mean for full angular distribution. The second type of map in the Fig. 10 B and C show radial and angular density (on X-Y plane) of osmolyte molecules relative to the axis of DNA helix and for this type of maps density values are calculated as a mean for all base pairs (DNA steps). As shown by the first density maps in Fig. 10B and C urea molecules form two solvating shell, outside and inside the DNA helix, while TMG forms one, but the well defined external solvating shell. This is due to the fact that urea molecules easily enter the minor and major groove, which causes that concentration of urea molecules in grooves is definitely higher that TMG molecules. This fact is confirmed by the second type of density maps presented in the Fig. 10 E and F. TMG molecules are more likely to accumulate around DNA backbone (outside of the DNA helix) than around nucleobases, while urea molecules enter the interior of the DNA helix. In addition, from the first type of density maps in the Fig. 10 E and F can be seen preference of TMG molecules to 3-rd, 8-th, 12-th and 15-th base pair, which corresponds to G-C or C-G in DNA sequence. While for urea molecules it is difficult to distinguish a particular preference.

3.10   Hydrogen bonds between DNA and osmolyte solutions

Information about the accumulations of molecules around DNA surface is not enough to determine whether osmolytes increase the solvation properties of the solution relative to the aqueous solution without osmolyte. Therefore, we calculated the number of hydrogen bonds formed by selected fragments of the DNA structure and osmolyte molecules (Fig. 11 A) and all molecules of the solution (Fig. 11 C) in 3.5M TMG and 3.5M urea solutions. We also determined changes in the number of
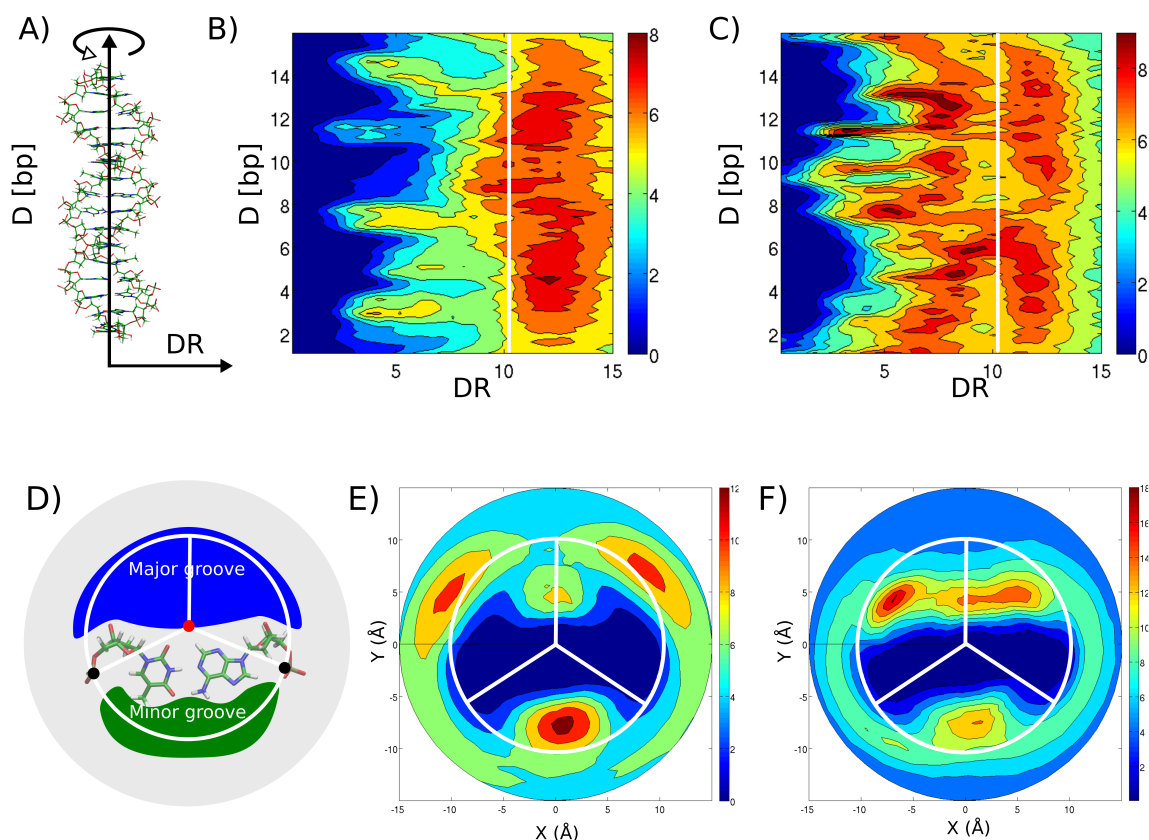
Figure 10: A) Definition of DR (radial distance from the axis of DNA helix) and D (distance along the helix axis, base pair index) helicoidal coordinates for 2-dimensional density maps. 2-dimensional density distribution of TMG B) and urea C) molecules around DNA in helicoidal coordinates, projection along the distance from the DNA helix axis and along the axis of DNA helix. The white line in B) and C) shows the position of phosphate groups relative to the axis of DNA helix and represents the radius of DNA helix. D) Alignment and definition of the X-Y plane coordinate system on the example of the G-C base pair for the second type of 2-dimensional density maps. The red dot represents the axis of DNA helix, black dots represent positions of phosphorus atoms, the white circle represents the radius of the DNA helix, green field represents the area of minor groove and blue field represents the area of major groove. Density distribution of TMG E) and urea F) molecules around DNA in 3.5 M solutions, density values calculated as mean for all base pairs.

hydrogen bonds during DNA denaturation in the same solutions (Fig. 11 B and D).

Fig. 11 A shows that in the native state of DNA TMG molecules do not form many hydrogen bonds with all kinds of nitrogen bases. What's more, we have not observed any hydrogen bonds with thymine residues and naturally with DNA backbone. In contrast, urea forms a lot of hydrogen bonds with whole DNA structure and in particular with DNA backbone.

Fig. 11 B shows that the denaturation of DNA significantly increases the number of hydrogen bonds of osmolyte molecules with DNA. However, in the denatured state of DNA, the biggest increase in the number of new hydrogen bonds have been observed for TMG molecules with guanine residues. For the other nitrogen bases, the increase is definitely smaller. Urea molecules in denatured state interact better with nitrogenous bases and in total forms more new hydrogen bonds with nitrogen bases than the DNA backbone.

Fig. 11 C shows that the best solvated fragment of the DNA structure is the backbone and this fact is independent of the type of solution. Presence of TMG molecules in solution causes weakening whole hydrogen bonding network between whole DNA and solution. The biggest reduction in solvation is observed for guanine, thymine and DNA backbone. Urea solution keeps the same level of solvation and for backbone, guanines and adenines even slightly higher.
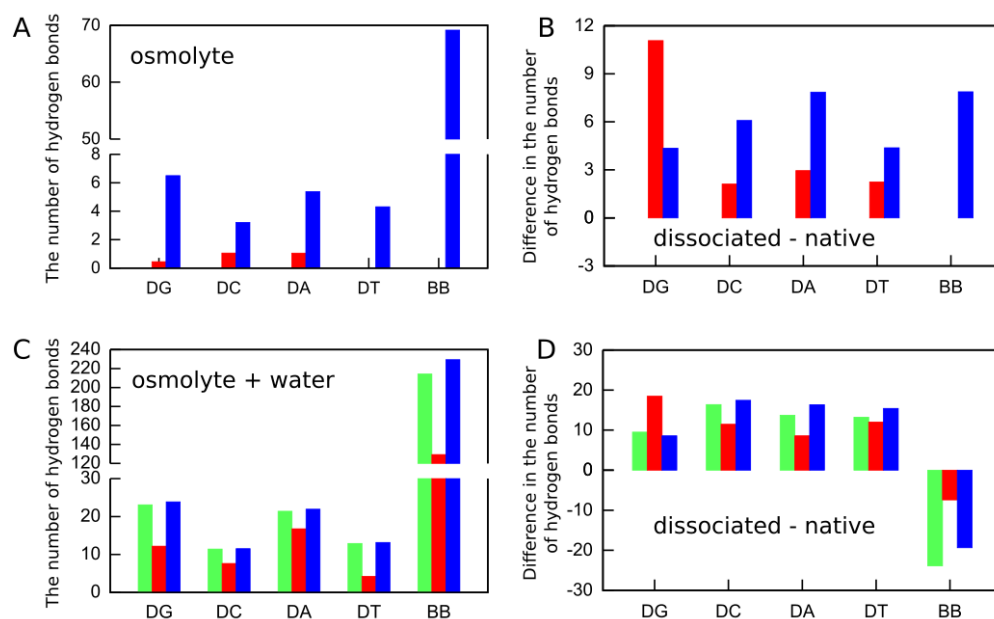
15

Figure 11: A) The number of hydrogen bonds of osmolyte with each nucleobase of DNA (DG, DC, DA, DT) and DNA backbone (BB) in the native state of DNA. B) The difference in the number of hydrogen bonds between osmolytes and different fragments of DNA during denaturation (difference between dissociated state and native state). C) The total number of hydrogen bonds of osmolyte solutions (water+osmolytes) with different fragments of DNA in the native state of DNA. D) The difference between the total number of hydrogen bonds in the dissociated state and native state. Data for the aqueous solution without osmolyte (green boxes), TMG 3.5 M (red bars) and urea 3.5 M (blue bars) systems.

Fig. 11 D shows that DNA denaturation is associated with significant decrease in solvation of DNA backbone for all solutions, however, betaine weakens this effect. For urea solution in the denatured state of DNA, the number of hydrogen bonds of cytosine, thymine and adenine residue is higher than in aqueous solution without osmolyte. Only for guanine solvation is smaller. TMG solution exhibits the opposite behavior. Changes of solvation between denatured and native state are positive, but definitely the most significant for guanines.

3.11 The energy of DNA interaction with solution molecules

Spontaneous denaturation of DNA is due to more favorable interactions between different parts of the system in a denatured state than in native state. Therefore, we have determined the main enthalpy driving forces of ctDNA denaturation into into contributions due to the energy of interactions between individual structural elements of the system. The contributions, shown in Fig. 12, involve both electro-static and van der Waals energies and were calculated by averaging the enthalpy differences between native and denatured states.

Fig. 12 shows that in aqueous solutions without osmolytes and urea solutions changes in the in-tramolecular interaction in DNA molecule (DNA–DNA) are strongly unfavorable during denaturation of DNA (1700–1850 kJ/mol), however, in betaine solutions this effect is definitely weaker (140–500 kJ/mol). It may be the result of subtle differences in conformational DNA in different solutions, es-pecially in denatured state. At this same time, denaturation of the DNA molecule causes an increase in the surface of DNA available for the solution and in consequence increasing the interaction of DNA with the solution. In fact, the sum of DNA interactions with water, osmolyte and Na ions is more favorable in the denatured state, however in TMG solutions denaturation due to the loss of DNA and Na ions interactions is strongly unfavorable. This is mainly due to the significant reduction of the number of Na ions around DNA by TMG molecules (see Fig. S2). The remaining interaction of Na ions with other parts of the system (WATER–NA, NA–NA, OSM–NA) also indicate a strong effect of
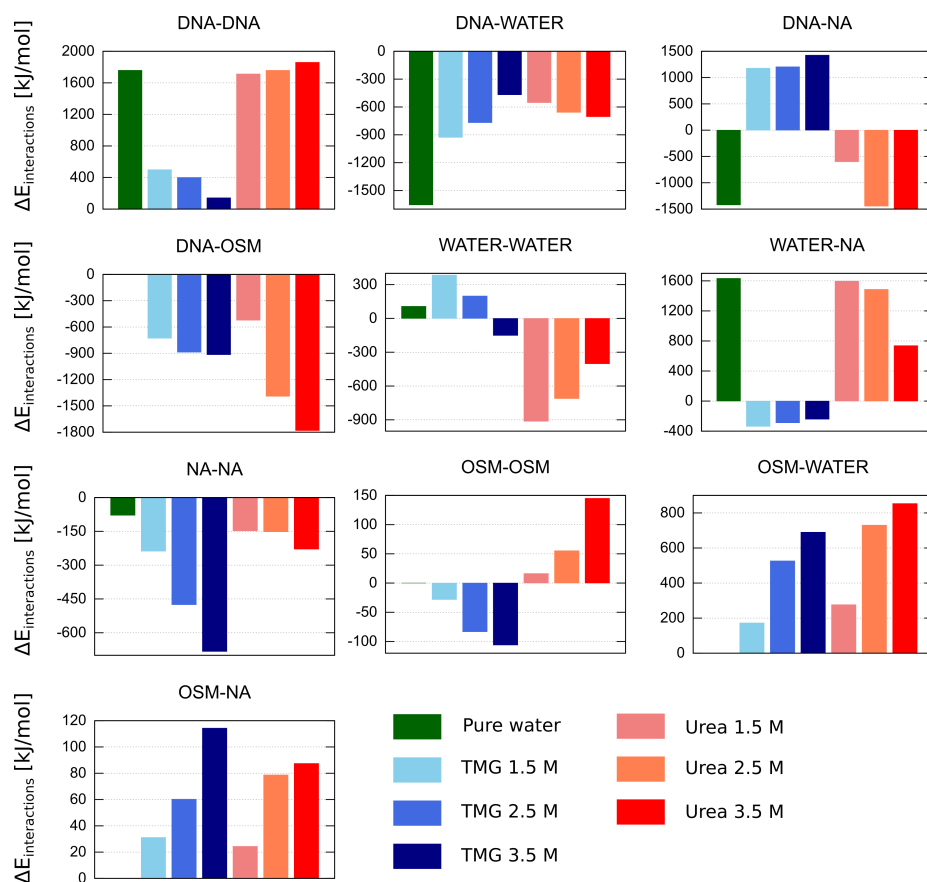
Figure 12: Values of energy interactions between different parts of simulated system (DNA, water, NA+ ions and osmolyte molecules) for TMG (blue bars) and urea solutions (red bars), calculated as difference of energy values in denatured state and native state. Negative values means increase of favorable interaction, and promotes denaturation. The color tone indicates the solution in which a given type of interaction occurs.

TMG molecules on the behavior of Na ions in the solution. In general, denaturation in the solutions without osmolytes and TMG solutions is a slightly unfavorable process for WATER–WATER interactions. Only in the urea solutions, the WATER–WATER interactions require significant reorganization (-400–900 kJ/mol), favoring denaturation. In contrast, the OSM–OSM interactions have completely opposite nature. More unfavorable interactions between urea molecules indicates an increase in contact between them and the release of urea molecules from the DNA surface in a denatured state. On the other hand, betaine molecules prefer to interact more with each other, which is reflected in the WATER-OSM interactions.

We have also determined the total enthalpy of denaturation of ctDNA in different solutions as the sum of all contributions from Fig. 12. Obtained by us value for aqueous solution (22 kJ/mol-bp) is very close to mean experimental value of enthalpy (28±2 kJ/mol bp) for ctDNA denaturation(59). For TMG solutions, this value are in the range 12–15 kJ/mol bp and 10–13 kJ/mol bp for TMG and urea solutions, respectively. Taking into account the mean experimental entropy for ctDNA denaturation (79.6±4 J/K mol-bp)(59) it results that the ctDNA in the aqueous solution in 300 K is stable (ΔG=-2 kJ/mol bp), as it is predicted by the experiment.

In the Fig. 13 we show the differences between osmolytes solution and solution without osmolytes for energy interactions of individual structural elements of the system. Not all contributions of energy interactions are shown due to the different number of water and osmolyte molecules in the systems.

Fig. 13 shows that adding osmolytes to the solution slightly enhances intramolecular interactions in DNA molecule (-10–60 kJ/mol), which is related to small conformational changes of DNA caused by the presence of osmolytes. In parallel, we observe a high loss in DNA-WATER energy interactions for
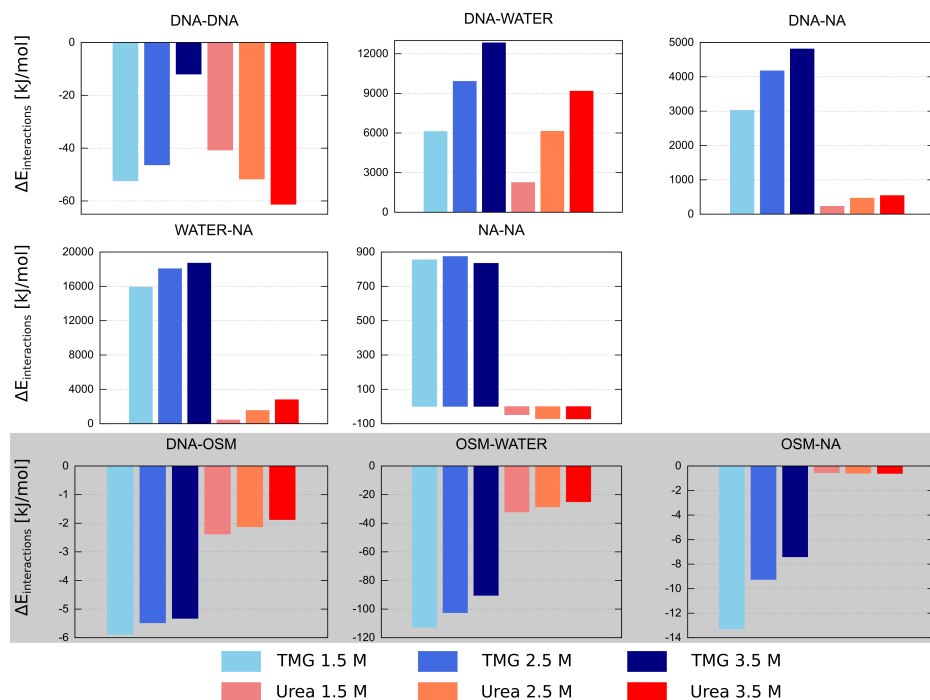
17

Figure 13: Values of energy interactions between different parts of the simulated system for TMG (blue bars) and urea solutions (red bars), calculated as the difference of energy values in osmolyte solution system and aqueous solution without osmolytes in native state. Negative values means an increase of favorable interaction. The color tone indicates the solution in which a given type of interaction occurs. In the gray rectangle at the bottom, are placed the values of the energy of interaction calculated per one mole of osmolyte particles.

both solutions (2500–13000 kJ/mol) and in DNA–NA energy interactions, especially for TMG solutions (3000-4800 kJ/mol). Moreover, after addition TMG to the solution, the NA–NA interactions become more unfavorable (850-900 kJ/mol), while after addition urea they become even slightly favorable (-50–100 kJ/mol).

Energy of NA–WATER interactions again, indicate large energy changes in the solution caused by osmolyte molecules, especially by TMG molecules. This indicates strong disorders in the interactions between Na ions and rest of the system, caused by the presence of TMG in solution. It turns out that strong changes in DNA–NA interaction are justified by the change in the number of Na ions around the DNA (see Fig. S2). Betaine molecules decrease the mean number of Na ions around the DNA (by 50–75%), causing a reduction in the overall stabilization of the DNA structure. Additionally, our DFT calculations show that TMG has a larger dipole moment than urea (15.4 D and 6.1 D, respectively). This additionally highlights the electrostatic nature of TMG–DNA interactions.

For the evaluation of our model, we also determined the enthalpy of direct interactions of osmolyte molecules with DNA, Na ions and water. The bottom panel in the Fig. 13 shows that interactions of osmolytes with the rest of the system compensated strongly unfavorable contributions presented above. Obtained by us enthalpy interactions of TMG molecules (-5.9–5.3 kJ/mol) and urea molecules with DNA (-2.4–1.9 kJ/mol) agree with experimental results above.

3.12   Changes in DNA conformation in the MD simulations

The structure of native double-stranded DNA is sensitive to solvent conditions, especially osmolytes activity. Here, we show analyses of conformational transition of DNA structure under the influence of osmolytes in our molecular dynamics simulations. We use X3DNA package(33) to calculate several geometric parameters describing the double helix in different solutions (see a list of geometrical parameters in SI section S.6). Next, we projected all data for all systems onto the plane formed by two first principal coordinates (vec1 and vec2 in the Fig.14A) obtained for the native state in the

aqueous solution without osmolyte using principal component analysis. We also determined geometric parameters that have the highest impact on the conformational transition of DNA structure.
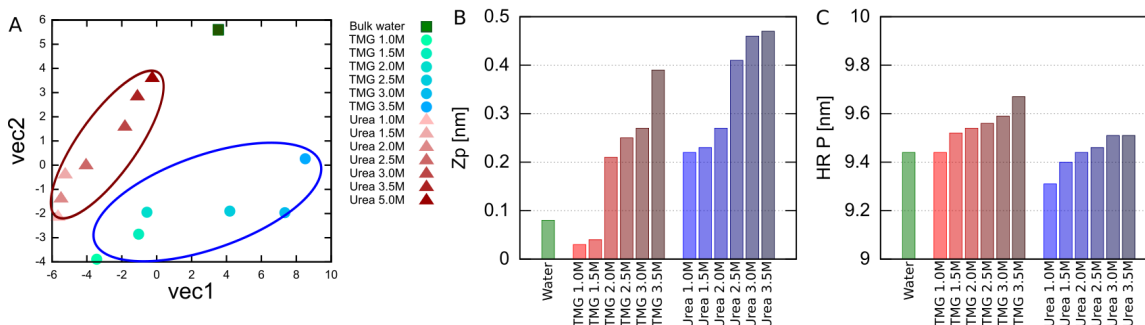

Figure 14: A) The data projection from different systems on the two first eigenvectors. Solutions with urea and betaine are well characterized by two first eigenvectors. B) Values of mean projection of the two phosphorus atoms onto the z-axis of the dimer 'middle frame' (Zp) and helical radius calculated from the position of P atoms (HR P) determined for DNA in the different solution of TMG and urea.

Fig.14 A depicting the conformational transition of DNA structure in pure water (green square), TMG solutions (blue circle) and urea solutions (red circle). As can be seen, in this projection the conformations adopted by DNA in solutions of both osmolytes are at a considerable distance from the conformation adopted by DNA in aqueous solution without osmolyte. Moreover, betaine and urea solutions show completely different conformational transitions in the DNA structure and depending on the concentration of solutions.

Fig.14 B and C show two parameters having the highest impact on DNA geometry. The big impact on a description of the DNA geometry has a position of the phosphate group relative to the mean base pair plane (Zp) and radius of double helix determined based on the positions of phosphors (HR P). The increasing value of Zp parameter in osmolyte solutions is the results the increasing distance between phosphorus atoms from DNA backbone. At the same time, helical radius (HR P) generally increases in osmolytes solutions. This local changes in DNA structure have an effect on the change of the length and diameter of the DNA, suggest that DNA undergo compression along helix axis. The values of these two parameters indicate a transition from B-DNA helix to A-DNA helix.

4 Conclusions

In our studies, we used experimental methods and MD simulations to explain the mechanisms responsible for denaturing of DNA by osmolytes. The most important conclusions from these studies are presented below:

The results of FTIR spectral studies and MD calculations indicate that the addition of TMG and urea to the aqueous solution cause dehydration of DNA with simultaneously occurring conformational changes of DNA molecule. Generally, this is a shift from the set of conformation of the type B towards the set of conformation of the type A. This effect is more pronounced in the case of TMG solutions. Addition of osmolytes to the aqueous solution are accompanied by nonmonotonic changes in many of the geometric parameters of the DNA characteristics. In particular, the length of hydrogen bonds between complementary bases is reduced, which may suggest an increase in the energy of the interaction. The distribution of hydrogen bonding angles indicates, however, that this may be the case only in TMG solutions.

The isolated vibrational spectra of osmolytes that have been affected by the presence of DNA in solution very little differ from the bulk osmolytes spectra. This may indicate that there is no direct specific interaction with DNA, or that the interaction of osmolytes with DNA is very similar to interacting with a water molecule. This conclusion seems to be confirmed by the results of the MD simulation. Both osmolytes are oriented preferentially with their positive poles of the dipole moment towards the surface of the DNA. In the case of TMG, this orientation indicates the small potential of this molecule to create specific interactions with nucleobases. However, this does not exclude completely the possibility of the interaction of both osmolytes with DNA through oxygen

19

atoms. This possibility is higher for urea molecules, and in the case of TMG it is more likely to be carried out by a water molecule.

Spatial distribution of osmolytes around the DNA molecule shows that urea forms two layers of molecules relative to the helix, one internal (in the large and the small DNA groove and between nucleobases) and outer (outside of the cylinder specified by the position of the phosphate groups). TMG shows only a well-defined outer layer, located along the backbone, however it does not accumulate along the nucleus.

Analysis of accumulation preference of osmolytes indicates that urea is generally more concentrated than TMG around all nucleotides and base pairs positions. The preference hierarchy is as follows: for urea occurs following series DG $\approx$ DC > DT > DA and for TMG DG > DT $\approx$ DC $\approx$ DA.

The calorimetric energy effects of DNA - osmolyte interactions are energetically negative, have small values (about -2.5$\pm$0.5 kJ/mol) and differ slightly in the case of TMG and urea. Theoretical analysis of the energy effects of the simulated systems leads to very similar values and shows strong compensating of large contribution to energy interactions from different components of the system.

The theoretical analysis of the interactions between the different components of system with DNA in native and dissociated state gives an insight into the mechanism of influence of both osmolytes on DNA stability. TMG and urea have a strong affinity to potential interaction sites of the single strand of DNA. TMG prefers interactions with guanidine, while urea interacts almost equally with all the bases. It is worth to point out to the system of strongly negative interactions energy of the dissociated DNA with both osmolytes.

TMG and urea are osmolytes having a different effect on protein stability, but having a similar destabilizing effect on the DNA. All indicates that the mechanism of their impact is different here. The strong affinity of both osmolytes to the nucleic bases appears to be the cause of their denaturing properties.

The result of the impact of various solutes, especially osmolytes, on DNA appears to be primarily a result of the balance of two main factors - the ability to neutralize of the negative charge of phosphate group of DNA helix and the affinity of the solute to the nucleic bases centers, blocked in the native state by hydrogen bonding between complementary bases.

5 Acknowledgement

References

[1] ADAMCZAK, B., WIECZÓR, M., KOGUT, M., STANGRET, J., AND CZUB, J. Molecular basis of the osmolyte effect on protein stability: a lesson from the mechanical unfolding of lysozyme. *Biochem. J. 473*, 20 (2016), 3705–3724.

[2] ARNOTT, S., AND SELSING, E. Structures for the polynucleotide complexes poly (dA)· poly (dT) and poly (dT)· poly (dA)· poly (dT). *Journal of molecular biology 88*, 2 (1974), 509–521.

[3] ASAKURA, S., AND OOSAWA, F. On interaction between two bodies immersed in a solution of macromolecules. *The Journal of Chemical Physics 22*, 7 (1954), 1255–1256.

[4] ASLANYAN, V. M., BABAYAN, Y. S., AND ARUTYUNYAN, S. G. Conformation and thermal stability of DNA in aqueous urea solutions. *Biophysics 29* (1984), 410–414.

[5] BABAYAN, Y. Conformation and thermostability of double-helical nucleic-acids in aqueous-solutions of urea. *MOLECULAR BIOLOGY 22*, 5 (1988), 962–967.

[6] BANYAY, M., SARKAR, M., AND GRÄSLUND, A. A library of IR bands of nucleic acids in solution. *Biophysical chemistry 104*, 2 (2003), 477–488.

[7] BARONE, G., VECCHIO, P. D., ESPOSITO, D., FESSAS, D., AND GRAZIANO, G. Effect of osmoregulatory solutes on the thermal stability of calf-thymus DNA. *Journal of the Chemical Society, Faraday Transactions 92*, 8 (Jan. 1996), 1361–1367.

[8] BECK, D. A., ALONSO, D. O., AND DAGGETT, V. A microscopic view of peptide and protein solvation. *Biophysical chemistry 100*, 1-3 (2002), 221–237.

[9] BRUŹDZIAK, P., ADAMCZAK, B., KACZKOWSKA, E., CZUB, J., AND STANGRET, J. Are stabilizing osmolytes preferentially excluded from the protein surface? FTIR and MD studies. *Physical Chemistry Chemical Physics 17*, 35 (2015), 23155–23164.

[10] BRUŹDZIAK, P., PANUSZKO, A., AND STANGRET, J. Chemometric determination of solute-affected solvent vibrational spectra as a superior way of information extraction on solute solvation phenomena. *Vibrational Spectroscopy 54*, 1 (2010), 65–71.

[11] BRUŹDZIAK, P., PANUSZKO, A., AND STANGRET, J. Influence of osmolytes on protein and water structure: a step to understanding the mechanism of protein stabilization. *The Journal of Physical Chemistry B 117*, 39 (2013), 11502–11508.

[12] BRUŹDZIAK, P., RAKOWSKA, P. W., AND STANGRET, J. Chemometric method of spectra analysis leading to isolation of lysozyme and CtDNA spectra affected by osmolytes. *Applied spectroscopy 66*, 11 (2012), 1302–1310.

[13] CANCHI, D. R., AND GARCÍA, A. E. Cosolvent effects on protein stability. *Annual review of physical chemistry 64* (2013), 273–293.

[14] CHALIKIAN, T. V., PLUM, G. E., SARVAZYAN, A. P., AND BRESLAVER, K. J. Influence of Drug Binding on DNA Hydration: Acoustic and Densimetric Characterizations of Netropsin Binding to the Poly (dAdT). cntdot. Poly (dAdT) and Poly (dA). cntdot. Poly (dT) Duplexes and the Poly (dT). cntdot. Poly (dA). cntdot. Poly (dT) Triplex at 25. degree. C. *Biochemistry 33*, 29 (1994), 8629–8640.

[15] COLASANTI, A. V., LU, X.-J., AND OLSON, W. K. Analyzing and building nucleic acid structures with 3dna. *Journal of visualized experiments: JoVE*, 74 (2013).

[16] DI MICHELE, A., FREDA, M., ONORI, G., PAOLANTONI, M., SANTUCCI, A., AND SASSI, P. Modulation of hydrophobic effect by cosolutes. *The Journal of Physical Chemistry B 110*, 42 (2006), 21077–21085.

[17] FALK, M., HARTMAN, K. A., AND LORD, R. C. Hydration of deoxyribonucleic acid. III. A spectroscopic study of the effect of hydration on the structure of deoxyribonucleic acid. *Journal of the American Chemical Society 85*, 4 (1963), 391–394.

[18] FOLOPPE, N., AND MACKERELL JR, A. D. All-atom empirical force field for nucleic acids: I. Parameter optimization based on small molecule and condensed phase macromolecular target data. *Journal of computational chemistry 21*, 2 (2000), 86–104.

[19] FRANKLIN, R. E., AND GOSLING, R. G. The structure of sodium thymonucleate fibres. I. The influence of water content. *Acta Crystallographica 6*, 8-9 (1953), 673–677.

[20] FUJIMOTO, S., AND YANG-XIN, Y. Effect of electrolyte concentration on DNA A–B conformational transition: An unrestrained molecular dynamics simulation study. *Chinese Physics B 19*, 8 (2010), 088701.

[21] FUNKNER, S., HAVENITH, M., AND SCHWAAB, G. Urea, a structure breaker? answers from thz absorption spectroscopy. *The Journal of Physical Chemistry B 116*, 45 (2012), 13374–13380.

[22] GUINN, E. J., PEGRAM, L. M., CAPP, M. W., POLLOCK, M. N., AND RECORD, M. T. Quantifying why urea is a protein denaturant, whereas glycine betaine is a protein stabilizer. *Proceedings of the National Academy of Sciences* (2011).

[23] HESS, B. P-LINCS: A parallel linear constraint solver for molecular simulation. *Journal of Chemical Theory and Computation 4*, 1 (2008), 116–122.

[24] Hess, B., Kutzner, C., Van Der Spoel, D., and Lindahl, E. GROMACS 4: algorithms for highly efficient, load-balanced, and scalable molecular simulation. *Journal of chemical theory and computation 4*, 3 (2008), 435–447.

[25] Hong, J., Capp, M. W., Anderson, C. F., Saecker, R. M., Felitsky, D. J., Anderson, M. W., and Record, M. T. Preferential interactions of glycine betaine and of urea with DNA: implications for DNA hydration and for effects of these solutes on DNA stability. *Biochemistry 43*, 46 (2004), 14744–14758.

[26] Ivanov, V., Minchenkova, L. E., Schyolkina, A. K., and Poletayev, A. I. Different conformations of double-stranded nucleic acid in solution as revealed by circular dichroism. *Biopolymers 12*, 1 (1973), 89–110.

[27] Ivanov, V. I., Minchenkova, L. E., Burckhardt, G., Birch-Hirschfeld, E., Fritzsche, H., and Zimmer, C. The detection of B-form/A-form junction in a deoxyribonucleotide duplex. *Biophysical journal 71*, 6 (1996), 3344–3349.

[28] Jorgensen, W. L., Chandrasekhar, J., Madura, J. D., Impey, R. W., and Klein, M. L. Comparison of simple potential functions for simulating liquid water. *The Journal of chemical physics 79*, 2 (1983), 926–935.

[29] Kim, Y., Geiger, J. H., Hahn, S., and Sigler, P. B. Crystal structure of a yeast TBP/TATA-box complex. *Nature 365*, 6446 (1993), 512–520.

[30] Kinne, R. K. The role of organic osmolytes in osmoregulation: from bacteria to mammals. *Journal of Experimental Zoology Part A: Ecological Genetics and Physiology 265*, 4 (1993), 346–355.

[31] Klump, H., and Burkart, W. Calorimetric measurements of the transition enthalpy of DNA in aqueous urea solutions. *Biochimica et Biophysica Acta (BBA)-Nucleic Acids and Protein Synthesis 475*, 4 (1977), 601–604.

[32] Kopka, M. L., Yoon, C., Goodsell, D., Pjura, P., and Dickerson, R. E. The molecular origin of DNA-drug specificity in netropsin and distamycin. *Proceedings of the National Academy of Sciences 82*, 5 (1985), 1376–1380.

[33] Lu, X.-J., and Olson, W. K. 3dna: a software package for the analysis, rebuilding and visualization of three-dimensional nucleic acid structures. *Nucleic acids research 31*, 17 (2003), 5108–5121.

[34] Malinowski, E. R. Obtaining the key set of typical vectors by factor analysis and subsequent isolation of component spectra. *Analytica Chimica Acta 134* (1982), 129–137.

[35] Malinowski, E. R. *Factor analysis in chemistry*. Wiley, 2002.

[36] Miner, J. C., and García, A. E. Equilibrium denaturation and preferential interactions of an rna tetraloop with urea. *The Journal of Physical Chemistry B 121*, 15 (2017), 3734–3746.

[37] Miyamoto, S., and Kollman, P. A. SETTLE: an analytical version of the SHAKE and RATTLE algorithm for rigid water models. *Journal of computational chemistry 13*, 8 (1992), 952–962.

[38] Miyoshi, D., and Sugimoto, N. Molecular crowding effects on structure and stability of DNA. *Biochimie 90*, 7 (July 2008), 1040–1051.

[39] Mohr, S. C., Sokolov, N. V., He, C. M., and Setlow, P. Binding of small acid-soluble spore proteins from Bacillus subtilis changes the conformation of DNA from B to A. *Proceedings of the National Academy of Sciences 88*, 1 (1991), 77–81.

[40] Nakano, S.-i., Miyoshi, D., and Sugimoto, N. Effects of Molecular Crowding on the Structures, Interactions, and Functions of Nucleic Acids. *Chemical Reviews 114*, 5 (Mar. 2014), 2733–2758.

[41] Nishimura, Y., Torigoe, C., and Tsuboi, M. Salt induced B—A transition of poly (dG). poly (dC) and the stabilization of A form by its methylation. *Nucleic acids research 14*, 6 (1986), 2737–2748.

[42] Panuszko, A., Bruździak, P., Kaczkowska, E., and Stangret, J. General Mechanism of Osmolytes' Influence on Protein Stability Irrespective of the Type of Osmolyte Cosolvent. *The Journal of Physical Chemistry B 120*, 43 (2016), 11159–11169.

[43] Piasek, Z., and Urbanski, T. The infra-red absorption spectrum and structure o f urea. *B Pol Acad Sci-Tech X* (1962), 113–120.

[44] Pilet, J., and Brahms, J. Dependence of BA conformational change in DNA on base composition. *Nature 236*, 65 (1972), 99–100.

[45] Pohl, F. M. Polymorphism of a synthetic DNA in solution. *Nature 260*, 5549 (1976), 365–366.

[46] Rajendrakumar, C. S., Suryanarayana, T., and Reddy, A. R. DNA helix destabilization by proline and betaine: possible role in the salinity tolerance process. *FEBS letters 410*, 2-3 (1997), 201–205.

[47] Record Jr, M. T., Zhang, W., and Anderson, C. F. Analysis of effects of salts and uncharged solutes on protein and nucleic acid equilibria and processes: a practical guide to recognizing and interpreting polyelectrolyte effects, Hofmeister effects, and osmotic effects of salts. *Advances in protein chemistry 51* (1998), 281.

[48] Rees, W. A., Yager, T. D., Korte, J., and Von Hippel, P. H. Betaine can eliminate the base pair composition dependence of DNA melting. *Biochemistry 32*, 1 (1993), 137–144.

[49] Saenger, W. Structure and dynamics of water surrounding biomolecules. *Annual review of biophysics and biophysical chemistry 16*, 1 (1987), 93–114.

[50] Saenger, W. *Principles of nucleic acid structure.* Springer Science & Business Media, 2013.

[51] Saladino, G., Pieraccini, S., Rendine, S., Recca, T., Francescato, P., Speranza, G., and Sironi, M. Metadynamics study of a β-hairpin stability in mixed solvents. *Journal of the American Chemical Society 133*, 9 (2011), 2897–2903.

[52] Sapir, L., and Harries, D. Origin of enthalpic depletion forces. *The journal of physical chemistry letters 5*, 7 (2014), 1061–1065.

[53] Schwinefus, J. J., Kuprian, M. J., Lamppa, J. W., Merker, W. E., Dorn, K. N., and Muth, G. W. Human telomerase RNA pseudoknot and hairpin thermal stability with glycine betaine and urea: Preferential interactions with RNA secondary and tertiary structures. *Biochemistry 46*, 31 (2007), 9068–9079.

[54] Singh, L. R., Poddar, N. K., Dar, T. A., Kumar, R., and Ahmad, F. Protein and DNA destabilization by osmolytes: the other side of the coin. *Life sciences 88*, 3 (2011), 117–125.

[55] Stumpe, M. C., and Grubmüller, H. Aqueous urea solutions: structure, energetics, and urea aggregation. *The Journal of Physical Chemistry B 111*, 22 (2007), 6220–6228.

[56] Texter, J. Nucleic acid-water interactions. *Progress in biophysics and molecular biology 33* (1979), 83–97.

[57] Tribello, G. A., Bonomi, M., Branduardi, D., Camilloni, C., and Bussi, G. Plumed 2: New feathers for an old bird. *Computer Physics Communications 185*, 2 (2014), 604–613.

[58] Tsuboi, M. Application of infrared spectroscopy to structure studies of nucleic acids. *Applied spectroscopy reviews 3*, 1 (1970), 45–90.

[59] Vaitiekunas, P., Crane-Robinson, C., and Privalov, P. L. The energetic basis of the DNA double helix: a combined microcalorimetric approach. *Nucleic acids research 43*, 17 (2015), 8577–8589.

[60] VANOMMESLAEGHE, K., HATCHER, E., ACHARYA, C., KUNDU, S., ZHONG, S., SHIM, J., DARIAN, E., GUVENCH, O., LOPES, P., VOROBYOV, I., AND A., M. D. Charmm general force field: A force field for drug-like molecules compatible with the charmm all- atom additive biological force fields. *J. Comput. Chem. 31*, 4 (2010), 671–690.

[61] WANG, Y., THOMAS, G. A., AND PETICOLAS, W. L. A duplex of the oligonucleotides d (GGGGGTTTTT) and d (AAAAACCCCC) forms an A to B conformational junction in concentrated salt solutions. *Journal of Biomolecular Structure and Dynamics 6*, 6 (1989), 1177–1187.

[62] WESTHOF, E. Water: an integral part of nucleic acid structure. *Annual review of biophysics and biophysical chemistry 17*, 1 (1988), 125–144.

[63] WHITE, A., AND JIANG, S. Local and bulk hydration of zwitterionic glycine and its analogues through molecular simulations. *The Journal of Physical Chemistry B 115*, 4 (2010), 660–667.

[64] YANCEY, P. H. Compatible and counteracting solutes: protecting cells from the Dead Sea to the deep sea. *Science progress 87*, 1 (2004), 1–24.

[65] YANCEY, P. H., BLAKE, W. R., AND CONLEY, J. Unusual organic osmolytes in deep-sea animals: adaptations to hydrostatic pressure and other perturbants. *Comparative Biochemistry and Physiology Part A: Molecular & Integrative Physiology 133*, 3 (2002), 667–676.

[66] YANCEY, P. H., CLARK, M. E., HAND, S. C., BOWLUS, R. D., AND SOMERO, G. N. Living with water stress: evolution of osmolyte systems. *Science 217*, 4566 (1982), 1214–1222.